Available online at www.sciencedirect.com
SCIENCE DIRECT
Coordination Chemistry Reviews 250 (2006) 844–854
COORDINATION CHEMISTRY REVIEWS
www.elsevier.com/locate/ccr

Review

Some aspects of actinide speciation by laser-induced spectroscopy

G. Geipel *

Institute of Radiochemistry, Forschungszentrum Rossendorf, P.O.Box 510119, D-01314 Dresden, Germany

Received 31 May 2005; accepted 18 November 2005
Available online 18 January 2006

Contents

Abstract

During the past decade many studies on speciation of actinides in natural and artificial environments have been carried out. High demands on the sensitivity in speciation of actinides lead to the development of advanced detection methods. This is connected with intensive use of laser systems as excitation sources. The laser can provide any wavelength from the near UV to the near infrared (NIR) wavelength range. The development of tunable solid-state lasers overcame some disadvantages of dye laser systems. The application of low temperatures for samples measured with fluorescence spectroscopic methods brought effort in the detection of carbonate species. The availability of modern femtosecond laser systems in combination with intensified charge coupled device (ICCD) cameras provided the possibility to exploit the fluorescence properties of aromatic organic compounds for the study of their interaction with actinides, especially non-fluorescent metal ions.

* Tel.: +49 351 260 2306; fax: +49 351 260 3553.
E-mail address: G.Geipel@fz-rossendorf.de.

0010-8545/$ – see front matter
doi:10.1016/j.ccr.2005.11.007

The fluorescence of some tetravalent actinides as Pa(IV) and U(IV) in aquatic systems have been described for the first time. The speciation of actinides in arsenate and several carbonate systems was investigated. The interaction with ligands from life sciences as adenosine triphosphate (ATP) and sugar phosphates became more and more important. Studies of the speciation of actinides in plants and microorganism also cannot be neglected.

In the solid-state the speciation of uranium(VI) in several natural and synthetic minerals has been studied as well as the behaviour of depleted uranium in the environment. The interaction of actinides with rock materials and minerals as well as their uptake is also of common interest in actinide chemistry. Especially the sorption and inclusion of Cm into several minerals lead to an improvement in knowledge of minor components in solids.

It is not possible to give a complete overview on the literature about the laser-induced spectroscopy of actinides. The restricted length of this contribution allows only a relatively small and personally influenced selection.

Keywords: Actinides; Laser-induced spectroscopy; Fluorescence; Photoacoustic

1. Introduction

In the field of laser-induced spectroscopy four main methods are used: laser-induced photoacoustic spectroscopy (LIPAS), laser-induced time-resolved fluorescence spectroscopy (TRLFS), ultra-short laser pulse-induced time-resolved fluorescence spectroscopy (fs-TRLFS), laser-induced breakdown detection and spectroscopy (LIBD/LIBS). All of these methods have been intensively developed during the last decades [1–8]. They became powerful tools to study interactions in solutions and at the solid–liquid interface. LIBD/LIBS concerns especially studies in colloidal systems. This theme is the aim of another contribution; therefore, it would be pardonable that LIBD is not treated here.

2. Recent development of methods

2.1. Laser-induced photoacoustic spectroscopy

Laser-induced photoacoustic spectroscopy (LPAS or LIPAS) and laser-induced thermal lensing spectroscopy were introduced in research on actinides in the eighties [3]. However, the thermal lens spectroscopy has not been applied very often due to its additional expenditure of a probe laser system for the detection of the thermal lens by light dispersion.

A very instructive overview on LIPAS is given by Kim [5]. Besides a general description of the method, information about the instrumentation and data processing is given. The solvent, mostly water, also generates a photoacoustic signal. Therefore, if measurements near the detection limit were carried out the spectra should be compensated with the spectrum of the solvent. The sensitivities of this method for various actinide elements in different oxidation states are also summarized. They depend on the molar absorbance. The speciation sensitivity is found to be $\alpha = 3 \times 10^{-6}\,\mathrm{cm}^{-1}$. With this value and the mostly known molar absorbance the concentration ranges for the lowest possible detection of actinides species in solution can be assessed.

Wruck et al. [9] used the collection of photoacoustic spectra at elevated temperature to estimate thermodynamic data in the system americium(III)-carbonate. As the photoacoustic signal depends on the temperature in the system a more lavish treatment of the data is necessary. Assuming that the absorption of all Am species in solution have the same factor function for the dependence on temperature at least the concentration ratio ($[AmCO_3^+]/[Am^{3+}]$ could be calculated from the spectra obtained. The absorption maximum for Am^{3+} is located at 503 nm and shifts to 505 nm for the $AmCO_3^+$ complex. The agreement of the calculated stability constant at 25 °C with data in the database [10] is within the error limits. Applying the van't Hoff relation for the temperature dependence of the stability constants the enthalpy change for the formation of $AmCO_3^+$ could be derived. The determined equilibrium constants for the reaction:

$$Am^{3+} + CO_3^{2-} \Leftrightarrow AmCO_3^+ \quad (1)$$

range from $\log \beta_1 = 6.26 \pm 0.12$ to $\log \beta_1 = 7.54 \pm 0.43$ in the temperature interval 25–75 °C. From these data the reaction enthalpy was estimated to be 37 ± 11 kJ/mol.

Several studies have been done on the interaction of americium with humic substances by LIPAS [11–13]. However, as the structure of the humic substances is much less known than with other ligands, these types of compounds will be not considered here.

During the last years only a few publications using laser-induced photoacoustic spectroscopy as detection method were used. This may be caused by the limited wavelength range of each single dye. During the last 15 years solid-state lasers have been developed. These systems allow tuning the laser wavelength over wide ranges without large changes in the optical setup of the laser system [7]. Here LIPAS was used to validate the stability constant of $UO_2(CO_3)_3^{4-}$ at low concentrations. As this complex does not show fluorescence properties at room temperature LIPAS is the only choice in spectroscopic methods to decrease the concentration of species in the solution.

Much less data exist about tetravalent actinide species. Some effort may be expected in the near future as some of these species show fluorescence properties (see also next section). However, here also the laser-induced photoacoustic spectroscopy may provide a way to obtain better thermodynamic data. Therefore, LIPAS was applied to the uranium(IV) phosphate and arsenate system [14]. Due to the strong hydrolysis of uranium(IV) only measurements in acid solutions could be carried out. As uranium(IV) shows at least three broad absorption bands in the wavelength range 620–680 nm a spectroscopic range of about 90 nm has to be scanned. Here the advantage of a tunable solid-state laser system with its wide tuning range is of importance as

no change of the laser setup is necessary during the measurement of the spectra. The absorption maxima of uranium(IV) at 629, 649 and 672 nm are shifted by the formation of the complexes to 645, 657 and 667 nm in the phosphate system. In the arsenate system absorption maxima are located at 645 and 663 nm. The complex formation equilibrium was assigned to be

$$U^{4+} + 2H^{+} + XO_4^{3-} \Leftrightarrow UH_2XO_4^{3+} \quad X = P;\ As \tag{2}$$

The stability constants were derived to be $\log \beta^0_{121} = 25.23 \pm 0.12$ for the phosphate system and $\log \beta^0_{121} = 23.94 \pm 0.08$ for the arsenate system, respectively.

One of the latest contributions on LIPAS was published by Mesmin et al. [15]. In this paper a very detailed description about the necessary equipment and possible data handling is given. The detection limit of this method is about two orders of magnitude lower if compared with conventional absorption spectrophotometry. However, the authors mention that the use of a joulemeter gives a value averaged over several laser pulses. This seems not to be correct, as modern powermeters can read the energy of each single laser pulse. The problem of these devices is in some cases the response time of the powermeter, and it can arise that only each second or third laser pulse is collected during the experiment. LIPAS was used to identify the mechanism of the precipitation of uranium(VI)–dioxalate–hexahydrate. The authors noted that the uranium(VI)–dioxalato complex is first formed in solution.

2.2. Fluorescence spectroscopy at low and elevated temperatures

Fluorescence properties are known to be dependent on the temperature of the system under investigation. Temperatures below the freezing point may decrease dynamic quenching effects. Samples can easily be cooled down to temperatures of 77 and 4.2 K by use of liquid nitrogen and liquid helium.

The uranium(VI)–carbonato complexes ($UO_2(CO_3)_2^{2-}$ and $UO_2(CO_3)_3^{4-}$) do not emit any fluorescence light at room temperature. The quenching effect of carbonate hinders the observation of the fluorescence spectra in these compounds [16]. The alkaline earth uranium(VI)–carbonato complexes are one exception to this rule [17–20]. Also it is known that the water molecules in the solvation shell contribute to the quenching effect [21].

However, at temperature of liquid nitrogen (LN_2) or liquid helium (LHe) the intensity and resolution of fluorescence spectra can be significantly improved due to the decrease of the quenching effect. Wang et al. [22], has shown that besides the silicates and phosphates the carbonates also show intense and well-resolved fluorescence spectra at LHe temperature. A strong increase in the fluorescence lifetime is also observed. For example, the fluorescence lifetime of the uranyl ion increases from 1.8 μs at room temperature to about 270 μs at LHe temperature. The fluorescence lifetime of the $UO_2(CO_3)_3^{4-}$ species reaches 880 μs. For the $Ca_2UO_2(CO_3)_3$ complex, an increase of the fluorescence lifetime of 40 ns to 1280 μs was found. Also for a $UO_2(HPO_4)_2^{2-}$ complex species, the fluorescence lifetime is listed at LHe temperature to be 560 μs and at room temperature to be 47 μs. As this species is not listed in the NEA database update [23] and in the NAGRA database [24,25] it is questionable that this species really does exist.

Also it could be shown that this method can be applied to solid samples. For example Wang et al. [26] has studied the inclusion of uranium in calcite. The observed spectra lead to the conclusion that the uranium(VI) is located in two distinct chemical environments. These spectra are in agreement with those obtained from uranium in calcite and aragonite. Fluorescence spectra obtained from sediments at the Hanford site have the same peak positions and intensities as these where calcium is substituted by uranium in calcite and aragonite. It was concluded uranium was co-precipitated within these carbonates. This may have implications for the solubility of uranium in contaminated areas.

The uranium(VI) speciation at elevated temperatures by TRLFS has been studied by Kimura et al. [27] and Kirishima et al. [28]. Fluorescence measurements were carried out in the temperature range 25–100 °C. The fluorescence decay constant ($1/\tau$) follows the Arrhenius equation. The activation energy for the several studied species were derived, but in some cases large variations were observed from other data in the literature.

2.3. Time-resolved fluorescence spectroscopy with fs-laser systems

It is known that neptunium and plutonium in all oxidation states as well as thorium does not show fluorescence properties. In the environment organic ligands (like humic and fulvic substances and wood degradation products) can often interact with actinides. Most of these organic systems contain benzene rings with delocalized π-electrons. These compounds show intense fluorescence properties. However, the fluorescence decay constant is rather high corresponding to a short fluorescence lifetime in the nanosecond and picosecond time-scale.

In order to exploit these properties for the study of the interaction of actinides with organic ligands a fluorescence spectrometer was developed, especially designed for the observation of short fluorescence lifetimes [8]. Normally, the complexes formed between heavy metal ions and organic ligands do not show any fluorescence. Therefore, only one fluorescent component in the solution can be expected. This behaviour is named static quenching effect. By use of the mass balance the concentrations of the non-fluorescent components can be calculated. As result the Stern–Volmer equation leads to the formation constant of the complex. Usually no time-resolved measurements are necessary for this. However, if a simultaneous dynamic quench effect occurs, the fluorescence intensity is additionally decreased. This would result in stability constants that are too high. The dynamic quenching effect influences both the intensity and the fluorescence lifetime. In order to eliminate this possible effect, time-resolved measurements should be carried out.

At first as example, the interaction of uranium(VI) with 2,3-dihydroxybenzoic acid was studied. In this case it is pos-

sible to use the fluorescence of uranium to validate the data obtained from the fluorescence of the ligand. The fluorescence lifetime for the $C_6H_3(OH)_2COO^-$ species was determined to be 375 ± 32 ps. It was found that a 1–1 complex is formed at pH values from 3.0 to 4.0. Examination of the pH dependence of the conditional formation constants let to the conclusion that two protons are removed from the ligand molecule during the complex formation. The chemical reaction can be assigned to be

$$UO_2^{2+} + C_6H_3(OH)_2COOH \Leftrightarrow C_6H_3(O)(OH)COO(UO2)^- + 2H^+ \quad (3)$$

From the measurements of the ligand a formation constant of $\log K_c = -3.11 \pm 0.16$ was derived. This value is rather high and may be explained by the formation of a chelate ring between the ligand and the metal ion. EXAFS studies on the formed complex give strong evidence for the formation of a complex with the two neighboured phenolic OH groups. This would also explain the release of the two protons, as studies with other dihydroxybenzoic acids (for example 2,5-dihydroxybezoic acid, [29,30]) show only a release of one proton. Analyzing the fluorescence of the uranyl ion the same complex formation stoichiometry was found. However, the data result in a formation constant of $\log K_c = -3.99 \pm 0.44$. The excited state reactions of the non-complexed ligand may be the reason for this difference.

This problem has also been pointed out by Billard and Lützenkirchen [31], especially with view to the excited states of lanthanides and actinides. However, most of the fluorescence measurements of uranium occur if the photochemistry is negligible. Then the majority of the excited species has decayed to the ground state before reactions in the excited state occur to any significant degree and the resulting decays are usually not mono-exponential.

As the treatment of fluorescence spectra containing emissions from excited state reactions for the evaluation of complex formation reactions has not been completely solved until now, this method was applied to a ligand that does not show such a reaction under the experimental conditions selected. At pH values above 5.0, 4-hydroxy-3-methoxybenzoic acid (vanillic acid) does not undergo excited state reactions. As evidence for the absence of excited state reactions the Stokes shift between the absorption and the corresponding fluorescence maximum should be about 5000 cm^{-1} [32]. Stokes shifts of about 4500 cm^{-1} were determined for both the monovalent and the divalent anion of 4-hydroxy-3-methoxybenzoic acid. Nevertheless in this work [33] the correction of inner filter effects [34], which may be caused by absorption of the incident laser beam and by absorption of emitted fluorescence signal by the sample itself, must be applied.

As uranium under these pH conditions is already partly hydrolyzed, the complex formation of neptunium(V) was studied. From time-resolved measurements the lifetime of the ligand $C_6H_3(OH)(OCH_3)COO^-$ was determined to be 290 ps. Graphical analysis of the determined species concentrations obtained from the fluorescence intensity of the non-complexed ligand lead to a 2:1 complex stoichiometry. This stoichiometry was also confirmed by applying the Stern–Volmer equation. Including the dissociation constant of the ligand the stability constant for the reaction:

$$2NpO_2^+ + C_6H_3(O)(OCH_3)COO^{2-} \Leftrightarrow (NpO_2)_2C_6H_3(O)(OCH_3)COO \quad (4)$$

was derived to be $\log \beta_{201} = 7.33 \pm 0.10$ at an ionic strength of 0.1 mol/L and 21 °C.

2.4. Data treatment

An overview of the recommended methods for the analysis of the fluorescence decay is given by Eaton [35]. Besides the discussion of the non-linear least square method the method of moments is described intensively. Some other methods (global analysis, transform methods, maximum entropy method) are only referred to shortly. For judgement for the goodness of the fit parameters, additional statistical parameters must be included. Additionally, we must also draw attention to some pitfalls. The most important here seem to be the correction of light scattering. This contribution must be removed by an appropriate subtraction algorithm. Of less importance seem to be effects caused by the wavelength-dependent time response of the instrument and polarization effects. The first one should be only of influence if PMT tubes are used. The latter may occur predominantly by excitation with polarized light and if the emission is of the same time-scale as the molecular motion in the medium, i.e. about 100 ps.

The review by Billard and Lützenkirchen [31] should be used as very important guide to handle the influence of physicochemical modifications of the solution on spectroscopic parameters. The influence of changing solvents, addition of supporting electrolytes as well as the temperature is discussed intensively. Additionally problems of energy transfer (Förster mechanism) are provided. The derivation of equilibrium constants from TRLFS measurements is described in a separate paragraph. As important issue the order of decay in relation to the number of species gives hints to the existence of possible changes of the equilibria in the excited state.

3. Studies of actinides in solution by time-resolved laser-induced fluorescence spectroscopy

In the series of the lower actinides the fluorescence properties of uranium(VI), americium(III) and curium(III) are well known and often used for speciation studies connected with coordination chemistry [4,36–40]. The fluorescence properties of protactinium(IV) and uranium(IV) have been reported recently. Publications dealing with the fluorescence of uranium(VI) and curium(III) are numerous, and therefore, only a few can be selected in order to show actual trends. Only little work has been performed on the fluorescence spectroscopy of americium. This may be due by the short fluorescence lifetime of this cation in aqueous solution [40].

3.1. Tetravalent actinides in solution

Recently the fluorescence properties of protactinium(IV) in aqueous solution was observed [41]. For the excitation a XeCl-Excimerlaser with a pulse duration of 24 ns was used with a wavelength of 308 nm. However, the excitation maximum lies in the range 278–290 nm depending on the used acid solution. Therefore, the excitation optimum could not be reached. The fluorescence lifetimes were observed in a range from 12.6 to 18.3 ns. It is rather complicated to deduce a fluorescence lifetime in this range, if the duration of the excitation pulse is of about the same value. Depending on the mineral acid added (H_2SO_4, HCl) hypsochromic shifts of the fluorescence emission were observed, if the spectra were compared with those in 5 M $HClO_4$. Detection limits of the order of 10^{-7} M were expected, so that studies in a submicromolar concentration range seem possible. As mentioned already for the fluorescence of uranium(IV) future studies will be performed to evaluate the fluorescence property for speciation measurements.

It has also been reported that uranium(IV) does show fluorescence properties [42] in aqueous solution. The excitation corresponds to the 5f–5f transition. The emission peaks could be assigned to individual electronic transitions in agreement with data derived from absorption spectra. The lifetime was determined to be shorter than 20 ns at room temperature. Shorter lifetimes could not be determined with respect to the applied laser source. Ten fluorescence emission bands were located at 289, 291, 318, 320, 335, 338, 345, 394, 409 and 525 nm. All of these emissions originate from the $^1S_0$ state, which is reached by absorbing light at 245 nm (40,820 cm^{-1}). The detection limit for fluorescence measurement of uranium(IV) is expected be of the order of 10^{-6} M. This would be in the same order as the detection limit of LIPAS measurements.

To confirm these results, additional measurements were performed [30]. By use of the Nd:YAG-pumped OPO tunable laser system the fluorescence lifetime at room temperature in 0.1 M perchloric acid was determined to be 2.7 ± 0.1 ns. Applications of this behaviour can be expected in the near future [42]. More detailed information about uranium(IV) fluorescence can be found in a recent contribution [43]. As by Kirishima et al. [42] the fluorescence lifetime of the tetravalent uranium at room temperature could not be determined; in this publication the lifetime at LN_2 temperature is 149 ns. The same measurements were performed in a solution of D_2O. Here the fluorescence lifetime was determined to be 198 ns also at LN_2 temperature. Also the first results on fluorescence properties with some inorganic ligands are reported (Cl^-: $\tau = 142.3$ ns, SO_4^{2-}: $\tau = 132.2$ ns). In contrast to the fluorescence of UO_2^{2+}, chloride ions do not quench the fluorescence of tetravalent uranium.

3.2. Hexavalent uranium species in solution

3.2.1. Hydrolysis

The hydrolysis of uranium(VI) is one of the basic reactions needed for the derivation of complex reactions with other ligands, especially in pH range above 3.5. uranium(VI) forms several mono and polynuclear species depending on pH and the uranium concentration. Some intensive studies were carried out by Meinrath et al. [44] and Kato et al. [45]. The stability constant of the dimer species $(UO_2)_2(OH)_2^{2+}$ is about 0.3 orders of magnitude different than the data recommended in the NEA database [23]. In the paper by Meinrath et al. and Kato et al., one discrepancy was found in the fluorescence lifetime of the non-complexed uranyl ion. The fluorescence lifetime in 0.1 M $HClO_4$ was reported to be 1.9 ± 0.2 μs. While in the study of the hydrolysis with different CO_2 partial pressures, a lifetime of 0.9 ± 0.3 μs was derived. No explanation for this behaviour was given. It is known that carbonate and probably also dissolved CO_2 quenches the fluorescence of the uranyl ion. However, if this occurs in the carbonate containing systems the fluorescence lifetime would depend on the concentration of the quencher.

Time-resolved fluorescence spectroscopy was also used by Eliet et al. [46] to study the hydroxo complexes of uranium(VI). The polynuclear species contribute appreciably to the fluorescence intensity in aqueous solutions. $UO(OH)_3^-$ predominates in the pH range 10–12. By deconvolution, the single fluorescence spectra of the several species and their fluorescence lifetimes were derived. This work was later [47] completed by a study at elevated temperatures in order to study the temperature dependence of the fluorescence lifetime.

3.2.2. Sulfates

In the case of sulfate complexation of the uranyl ion [48] different fluorescence lifetimes can be used to distinguish between several uranyl–sulfate species.

Moll et al. [49] have investigated the ternary UO_2^{2+}–SO_4^{2-}–OH^- system. Unfortunately, the data derived were not checked by fluorescence measurements.

3.2.3. Phosphates

Several studies have been performed on the interaction of uranium(VI) with phosphate by fluorescence spectroscopy. Some of the uranium(VI) phosphate species show very high quantum efficiencies, and therefore, the uranium phosphate system can be studied at very low concentrations.

Eliet et al. [46] reported about the fluorescence in alkaline solution. According to the change in the spectrum phosphate species still exist under these conditions and a revision of the thermodynamic data for phosphate species at high pH is necessary. The possibility for the detection of the uranium(VI)–phosphate complexes ($UO_2H_2PO_4^+$, $UO_2(HPO_4)$(aq.), $UO_2PO_4^-$ in solution was reported by Scapolan et al. [50]. The spectroscopic data and fluorescence lifetimes were determined.

Brendler et al. [51] has studied the complex formation of uranium(VI) with phosphate at low concentrations by TRLFS. A wavelength of 355 nm was used to excite the species in solution. At this wavelength relatively low excitation of all uranium(VI) species occur. Therefore, the sensitivity under these conditions is very limited. Nevertheless the data, especially for the first complex $UO_2(HPO_4)$(aq.) is in excellent agreement with the data selected by the NEA database [23].

A very new study on phosphate complexation was carried out by De Pablo et al. [52]. They studied the fluorescence proper-

ties in the uranium(VI)–phosphate system in the pH range 1–5. Five different species could be identified. Besides the UO_2^{2+} ion, spectra were assigned to the species $UO_2(H_2PO_4)_2$(aq.), $UO_2H_2PO_4^+$, $UO_2(HPO_4)$(aq.) and $UO_2PO_4^-$. The spectra of $UO_2(H_2PO_4)_2$(aq.) and $UO_2H_2PO_4^+$ could not be resolved. However, by lifetime analysis the two species could be clearly detected. In this work the authors use a different procedure to determine the fluorescence intensity of different phosphate species in solution. The delay range was divided into several step ranges. Due to this it was possible to determine species with short lifetimes in the first measurement and species with long lifetimes in a separate measurement with a later start time after the laser pulse and also with a second longer exposure time of the CCD camera.

3.2.4. Organic phosphates

Fluorescence measurements were used to study the complex formation between uranium and adenosine 5′-triphosphate (ATP) [53]. The increase of fluorescence intensity is of the same order as for diphosphate ions. The emission bands also show a strong bathochromic shift. This indicates that the phosphate chain of the ATP molecule is responsible for the complex formation. However, the organic part of the ATP acts as a quencher for the fluorescence of the uranyl ion. Therefore, the fluorescence intensity detected and lifetime as function of the ATP concentration runs through a maximum. For the determination of stability constants the fluorescence intensities have to be corrected for the dynamic quenching effect by use of the Stern–Volmer equation. The stability constant for the UO_2ATP^- complex was $\log \beta_{11} = 7.44 \pm 0.44$.

Recently complex formation between uranium(VI) and α-D-glucose-1-phosphate has been studied [54]. In contrast to ATP complex formation here it was concluded that the formed α-D-glucose-1-phosphate complex does not emit any fluorescence. However, this behaviour seems to be in agreement with observations from adenosine-monophosphate (AMP) [53]. Due to this it was only possible to follow the 1:1 complex formation of uranium with α-D-glucose-1-phosphate. By potentiometric titration experiments it could be shown that a 1:2 complex is also formed at higher pH values. The stability constant of the 1:1 complex according to the reaction:

$$UO_2^{2+} + C_6H_{11}O_6PO_3^{2-} \Leftrightarrow UO_2(C_6H_{11}O_6PO_3) \quad (5)$$

was $\log \beta_{11} = 5.72 \pm 0.12$. This value is somewhat higher than that derived from potentiometric titrations ($\log \beta_{11} = 5.40 \pm 0.25$). This difference leads to an increase for the fraction of the $UO_2(C_6H_{11}O_6PO_3)$ complex in the speciation diagram of about 15% at the maximum by use of the TRLFS data. However, the fraction of the complex formed dominates the speciation diagram, if the concentration of the ligand reaches the 10-fold excess compared to the metal ion.

Additionally the complexation of uranium(VI) with glycerol 1-phosphate was studied by Koban and Bernhard [55] at pH 4.0 by use of TRLFS. The complex stability of $\log \beta_{11} = 6.15 \pm 0.05$ (ionic strength 0.1 M) for the reaction:

$$UO_2^{2+} + C_3H_7O_3PO_3^{2-} \Leftrightarrow UO_2(C_3H_7O_3PO_3) \quad (6)$$

is in good agreement with data obtained from potentiometric titrations ($\log \beta_{11} = 6.23 \pm 0.09$). The fluorescence lifetime for the complex formed was 155 ± 30 ns, which seems to be rather short for phosphate containing species. However, as the other complexes of the uranyl ion with organic monophosphates also did not show fluorescence properties, it seems that the fluorescence properties of uranium(VI) with organic phosphates depend on the structure of the ligand. In a third study, fluorescence spectroscopy was applied to obtain the interaction of uranium with sugar phosphates in solutions [56]. Glucose 6-phosphate and fructose 6-phosphate were used as ligands. In case of the glucose 6-phosphate a decrease of the fluorescence intensity was observed. The conclusion was drawn that the complex formed does not show fluorescence properties, as is also the case for the α-D-glucose-1-phosphate complex. In contrast if the fructose 6-phosphate complex is formed fluorescence properties can be measured. Compared to the non-complexed uranyl ion a bathochromic shift of about 325 cm^{-1} was measured in the wavelength range 480–545 nm. However, the fluorescence lifetime is again very short and amounts to 130 ± 50 ns. This is of the same order as for the glycerol 1-phosphate complex and also the shift in the fluorescence spectrum is comparable. Considering a uranium–phosphate bond the short fluorescence lifetime can be explained only by quench effects of the organic strain of the ligand.

The formation constants from fluorescence measurements at an ionic strength of 0.1 M and 25 °C yielded $\log \beta_{11} = 6.35 \pm 0.28$ for the glucose 6-phosphate complex and $\log \beta_{11} = 5.66 \pm 0.17$ for the fructose 6-phosphate complex, respectively.

3.2.5. Arsenates

Uranium forms several complex species with phosphate ions in solution. It can be expected that the homologous element arsenic form complexes in the same manner. Time-resolved fluorescence spectroscopy shows that several of these complexes exist [57]. The species $UO_2H_2AsO_4^+$, $UO_2(HAsO_4)$(aq.) and $UO_2(H_2AsO_4)_2$(aq.) were detected in solution with stability constants derived by deconvolution of the fluorescence spectra. The fluorescence lifetimes of the several species are also different from each other so the fit of the data to obtain the fluorescence decay value is multi-exponential. To assign the fluorescence spectra to the solution species in case of the $UO_2(HAsO_4)$(aq.) species a comparison with the fluorescence spectrum of the mineral troegerite was used and the fluorescence spectrum of $UO_2(H_2AsO_4)_2$(aq.) by comparison with the synthetic compound $UO_2(H_2AsO_4)_2 \cdot 1H_2O$.

Comparison of the $UO_2(HAsO_4)$ species is shown in Fig. 1. Within the error limit of the fluorescence measurements the agreement of the emission maxima between the several species is good.

The stability constants derived from TRLFS measurements are somewhat smaller than for the corresponding phosphate species. Comparison of the fluorescence spectra obtained by pH titration of a tailing water from a uranium mining facility gave evidence for the existence of these species under slightly acid environmental conditions [58].

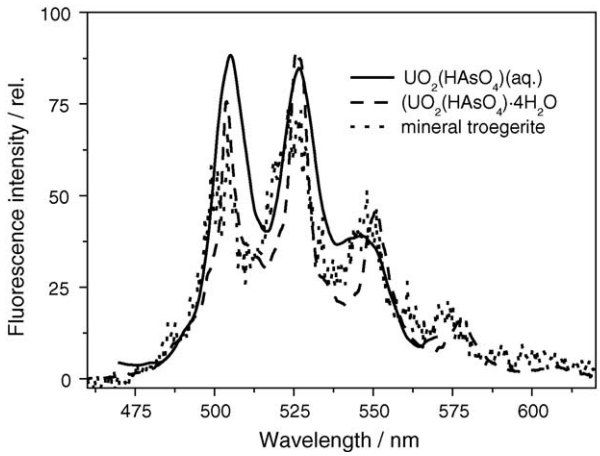

Fig. 1. Comparison of the several species of the $UO_2(HAsO_4)$ type.

3.2.6. Carbonates

Several papers have been published in the past decade concerning the interaction of carbonate with uranium(VI). Especially since the first description of the fluorescence properties of the $Ca_2UO_2(CO_3)_3$(aq.) species [17] several other publications followed [18–20,59,60]. The alkaline earth uranyl carbonates show relatively slight fluorescence emission with a short fluorescence lifetime in the range below 100 ns. The emission maxima show a hypsochromic shift compared to the uranyl ion. If compared to the spectrum of the $UO_2(CO_3)_3^{4-}$ species at low temperatures [20] the shift remains slightly bathochromic.

3.3. Trivalent species in solution — americium

Few studies of the fluorescence of americium have been performed. To determine the number of water molecule in the first solvation shell the fluorescence decay time can be used. This was already shown by Horrocks and Sudnick [61] for lanthanides. They found a direct proportionality between the luminescence decay constant and the number of coordinated water molecules in several europium(III) and terbium(III) complexes. Kimura and Kato have published an equation that connects the fluorescence decay constant ($1/\tau$) with the number of water molecules in the solvation shell of Am(III) assuming a number of nine water in pure aqueous solution [62]:

$$N_{H_2O} = 2.56 \times 10^{-7}\, k_{obs}\,(\mathrm{Am}) - 1.43 \quad k_{obs}\ \mathrm{in\ s^{-1}} \tag{7}$$

3.4. Trivalent species in solution — curium

Similar to Am the correlation between the number of water molecules in the hydration shell of Cm and the fluorescence decay constant is [63]:

$$N_{H_2O} = 6.5 \times 10^{-4}\, k_{obs}\,(\mathrm{Cm}) - 0.88 \quad k_{obs}\ \mathrm{in\ s^{-1}} \tag{8}$$

3.4.1. Hydrolysis

The hydrolysis of curium has been studied by TRLFS, as this technique is the most applicable method at low concentrations. Wimmer et al. [38] report the hydrolysis constants in 0.1 M $NaClO_4$ solution to be $\log \beta_{11} = 6.67 \pm 0.18$ and $\log \beta_{12} = 12.06 \pm 0.28$ for the reactions:

$$Cm^{3+} + OH^- \Leftrightarrow Cm(OH)^{2+} \tag{9}$$

$$Cm^{3+} + 2OH^- \Leftrightarrow Cm(OH)_2{}^{+} \tag{10}$$

These data differ significantly from those reported earlier by other authors, who exploited conventional techniques such as extraction and electromigration. This may be due a shift in the equilibrium of the excited species [31].

Emission spectra of the hydrolysis products of curium have been obtained by deconvolution [64]. The emission maxima for $Cm(OH)^{2+}$ and $Cm(OH)_2{}^{+}$ are 598.7 and 603.5 nm, respectively. From the fluorescence intensities the formation constants are $\log \beta^\circ_{11} = 6.38 \pm 0.09$ and $\log \beta^\circ_{12} = 12.3 \pm 0.2$. However, for the same reasons as mentioned above there may be differences with other methods.

3.4.2. Sulfates

By time-resolved fluorescence spectroscopy three curium–sulfate species could be identified [65]. The species are assigned to be $Cm(SO_4)^+$, $Cm(SO_4)_2{}^-$ and $Cm(SO_4)_3{}^{3+}$. Fluorescence emission maxima of these species are located at 596.2, 599.5 and 602.2 nm, respectively. At an ionic strength of 3 mol/kg the formation constants for

$$Cm^{3+} + SO_4{}^{2-} \Leftrightarrow Cm(SO_4)^+ \tag{11}$$

$$Cm^{3+} + 2SO_4{}^{2-} \Leftrightarrow Cm(SO_4)_2{}^- \tag{12}$$

are $\log \beta_{11} = 0.93 \pm 0.08$ and $\beta_{12} = 0.61 \pm 0.08$. The third species is estimated only at a high sulfate concentration above 1 mol/kg sulfate.

3.4.3. Phosphates

Several inorganic ligands such as OH^-, $CO_3{}^{2-}$, $H_2PO_4{}^-$, $HSiO_4{}^-F^-$, $HCO_3{}^-SO_4{}^{2-}$ and Cl^- can be found in brine solutions. Fanghänel et al. [66] gives an overview on the complex formation of Cm(III) with inorganic ligands. The ion-interaction coefficients to estimate the formation constants according to the Pitzer equation are included in this summary. This model can be used up to high salt concentrations of 6 mol/kg.

3.4.4. Organic phosphates

The interaction of curium with adenosine 5′-triphosphate was studied recently by Moll et al. [67] and performed at trace concentrations of curium (3.0×10^{-7} M), demonstrating the advantages of TRLFS methods. By deconvolution of the spectra at least three different solution species could be identified. These species differ only in the number of protons in the complex formed. The chemical reactions were assigned to be

$$Cm^{3+} + 2H^+ + ATP^{4-} \Leftrightarrow CmH_2ATP^+ \tag{13}$$

$$Cm^{3+} + H^+ + ATP^{4-} \Leftrightarrow CmHATP \tag{14}$$

$$Cm^{3+} + ATP^{4-} \Leftrightarrow CmATP^- \tag{15}$$

The stability constants derived from the fluorescence intensities for the species CmH_2ATP^+, CmHATP and $CmATP^-$ are $\log \beta_{121} = 16.86 \pm 0.09$, $\log \beta_{111} = 13.23 \pm 0.10$

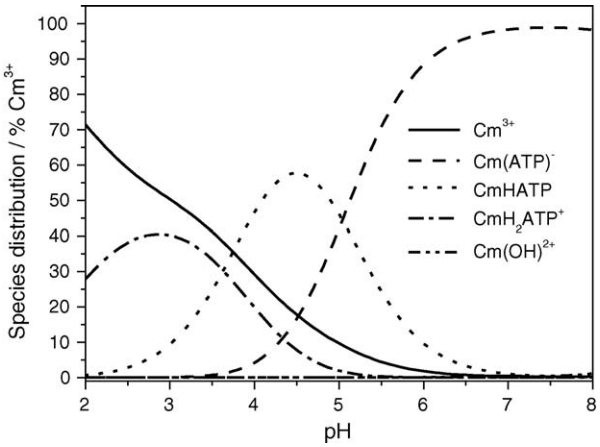

Fig. 2. Species distribution in the system Cm–ATP as function of pH (3×10^{-7} M Cm^{3+}, 3×10^{-6} M ATP, $I = 0.1$).

and $\log \beta_{101} = 8.19 \pm 0.16$, respectively. A calculated species distribution in the system Cm^{3+}–ATP as function of pH is shown in Fig. 2. The concentration of Cm^{3+} was set to be 3×10^{-7} M and the total concentration of ATP was 3×10^{-6} M. The ionic strength was 0.1 M. The speciation calculation was performed with the program "Species" [68]. Comparing this species distribution with a calculation performed for the NpO_2^+ system using the formation constants published by Rizkalla et al. [69], a similar behaviour is observed, where with increasing pH, complexes with a decreasing number of protons are formed and the amount of complexes increases, indicating a stronger complex formation in the series $CmH_2ATP^+ < CmHATP < CmATP^-$.

Including data from the fluorescence lifetime of the detected species and comparing this to the Eq. (8) derived by Kimura and Choppin [63], the number of water molecules in the solvation shell could be estimated. For the species CmH_2ATP^+ and CmHATP, a fluorescence lifetime of around 90 μs was found. This lifetime corresponds to six water molecules in the solvation shell. As the fluorescence lifetime is found to be in the range of inorganic phosphate complexes it was concluded that curium is bond in these two species to the partly deprotonated phosphate group. For the $CmATP^-$ species, a fluorescence lifetime of 187 μs was determined, which corresponds to an average of 2.6 coordinated water molecules. As this value is very low it is suggested that interactions to the nitrogen and the $–NH_2$ group of the adenine occur besides the phosphate chain. Comparing the stability constants with those derived for UO_2^{2+} [53] and NpO_2^+ [69], complex formation between actinides and ATP decreases in the following order:

$$Cm^{3+} > UO_2^{2+} \gg NpO_2^+$$

According to the effective charge of UO_2^{2+} of 3.2 [70] uranium should form the strongest complex in this series. However, steric effects of the uranyl ion may hinder the interaction of the metal ion with the ATP ligand [67].

3.4.5. Carbonates

Due to the excellent fluorescence properties of this actinide ion in solution, the chemistry of curium with carbonate has been studied intensively. The species $CmCO_3^+$, $Cm(CO_3)_2^-$ and $Cm(CO_3)_3^{3-}$ can be quantified by peak deconvolution of fluorescence spectra. However, there is also evidence for species formed with hydrogen carbonate ions [66,71]. For the reaction:

$$Cm^{3+} + H^+ + CO_3^{2-} \Leftrightarrow CmHCO_3^{2+} \quad (16)$$

the formation constant was $\log \beta^\circ_{111} = 1.9 \pm 0.2$ for the $Cm(HCO_3)^{2+}$. The formation constants for the other carbonate species $CmCO_3^+$, $Cm(CO_3)_2^-$, $Cm(CO_3)_3^{3-}$ and $Cm(CO_3)_4^{5-}$ according to the equation:

$$Cm^{3+} + nCO_3^{2-} \Leftrightarrow Cm(CO_3)_n^{(3-2n)+} \quad (17)$$

where n ranges from 1 to 4 are $\log \beta^\circ_{101} = 5.9 \pm 0.1$, $\log \beta^\circ_{102} = 10.27 \pm 0.3$, $\log \beta^\circ_{103} = 13.18 \pm 0.45$ and $\log \beta^\circ_{104} = 14.18 \pm 0.65$, respectively. The data show that hydrogencarbonate complex is formed to a small extent. As the study is performed in 1 mol/kg NaCl direct comparison with other data is not possible, also the formation of mixed hydroxo-carbonate species cannot be confirmed.

3.4.6. Other ligands

As mentioned already in the section on LIPAS of amercium the interaction of curium with humic substances will not be included in this contribution.

Organic ligands may show energy transfer reactions from the excited metal ion and vice versa if studied by fluorescence measurements. Such an intramolecular energy transfer in Cm^{3+} complexes is reported in [72]. At an excitation wavelength of 308 nm the fluorescence yield was increased by 77% for the phthalate and by 30% for the salicylate complex.

Klenze et al. [73] has studied the complex formation of 5-sulfosalicylic acid (H3SSA) with Cm(III). The complex formation of two complexes according to

$$Cm^{3+} + nO_3SC_6H_3(O)COO^{3-} \Leftrightarrow Cm(O_3SC_6H_3(O)COO)_n^{3(n-1)-}) \quad (18)$$

with $n = 1$ and 2 was found. At ionic strengths of 0.15 and 0.3 M the formation constants were $\log \beta_{101} = 6.44 \pm 0.03$ and $\log \beta_{102} = 11.99 \pm 0.04$ for the Cm(SSA) and $Cm(SSA)_2^{3-}$ complex, respectively. The formation constants did not show a dependence on the ionic strength of the solution.

4. Fluorescence spectroscopy of actinides in plants and microorganisms

Laser-induced fluorescence measurements were conducted to study the interactions of metal ions with living matter [74]. Panak et al. [74] studied the interaction of U(VI) with vegetative cells, heat killed cells, spores and decomposed cells of *Bacillus sphaericus*. The cells were decomposed in order to study the speciation of the uranium and additionally U(VI) was precipitated as $UO_2(H_2PO_4)_2$. The decomposed bacterial suspension showed the same fluorescence spectrum as $UO_2(H_2PO_4)_2$. Inner sphere complexes with organo-phosphate groups on the cell surface are formed.

Acidobacillus ferrooxidans is one of the most studied types of bacteria. The interaction with uranium(VI) was studied by Merroun et al. [75]. By measurement of the fluorescence lifetime of the bound uranium, three different fluorescence lifetimes were obtained. From this it was concluded that one complex should be stronger than the other two. However, no structural differences could by observed by EXAFS spectroscopy. The interpretation of these observations points to the fact that the same functional groups are implicated in the complex formation.

Günther et al. [76] published the first contribution on the direct determination of uranium species in plants. By use of TRLFS the change in the uranium speciation from the pore water of the soil of hydroponic solution to root, shoot axis and leaf of lupines was studied. However, due to the lack in fluorescence spectra of several phosphate compounds for comparison a clear distinction between inorganic and organic phosphate complexes could not yet drawn. The fluorescence spectra of the hydroponic solutions and the species detected in the plants differ significantly. In the hydroponic solutions uranyl hydroxo species dominate the speciation. This speciation is changed clearly to phosphate containing species proven by a shift in the fluorescence emission maxima.

Curium shows one of the highest fluorescence efficiency of the f-elements. Therefore, this property can be used to study the interaction of curium species with bacteria. The interaction of Cm(III) with *Bacillus subtilis* and *Halobacterium salinarum* shows K_d values from 1000 to 10,000 in the pH range 3.0–5.0 [77]. From the fluorescence lifetime, a change in the number of water molecules in the coordination sphere was derived. In the case of *Bacillus subtilis* a decrease was found with increasing pH, and in the case of *Halobacterium salinarum* an increase of the number of water molecules with increasing pH was shown. The authors conclude that the sorption on *Halobacterium salinarum* occurs in a more outer sphere fashion than for *Bacillus subtilis*.

The interaction of Cm with microorganisms has been studied by Moll et al. [78] by use of time-resolved laser-induced fluorescence spectroscopy. As excitation source the second harmonic of a flash lamp pumped Ti-sapphire laser was used. The fluorescence emission was measured with an intensified CCD-camera. The sulfate reducing bacterial strain *Desulfovibrio äspeöensis* forms by biosorption in an inner sphere surface complex. The parameters of the complex formed are an emission wavelength at 600.1 nm and a fluorescence lifetime of 162 ± 5 μs. Under the chosen experimental conditions no evidence for the incorporation of Cm into the bacterial cells was found. The complex formation already starts at a pH value of 3.0 and is reversible that could be shown by desorption experiments. The fluorescence lifetime in the pH range where the complex and free Cm^{3+} ions coexist in the solution follows biexponential decay behaviour. This indicates that no shift in the complex stability occurs in the excited state [79]. By use of Eq. (8) derived by Kimura and Choppin [63] the fluorescence lifetime of 162 μs indicates that three water molecules remain in the first solvation shell of the bound curium.

5. TRLFS on solids, minerals and synthetic minerals

Many of the uranium minerals show intense fluorescence properties. This can be used to identify these minerals by their fluorescence characteristics. Fluorescence spectra of synthetic liebigite and andersonite were published by Vochten et al. [80]. Later, spectra of synthetic soddyite and boltwoodite were measured [81,82]. The fluorescence properties including fluorescence decay times of some uranium phosphate and arsenate minerals were published by Geipel et al. [83]. The most intensive fluorescence emission is located between 500 and 530 nm and between the several differ minerals, differences are relatively small within about 5 nm. Larger differences have been found for the fluorescence lifetimes. Besides this, the spectra obtained from a mineral and its solution species are comparable.

In the case of some alkaline earth uranium(VI) carbonate minerals TRLFS was also used to identify spectroscopic differences between the several minerals species [20,84,85]. The minerals bequerelite and swartzite [84] differ completely from each other. As the bequerelite contains hydroxo ions the fluorescence is more comparable to the uranium(VI) hydroxo species than to alkaline earth uranium(VI) carbonates. The fluorescence spectrum of swartzite is very similar to the spectra of bayleyite, liebigite and andersonite as well as to the synthetic mineral $Ba_2[UO_2(CO_3)_3] \times 6H_2O$ [20]. The spectrum of the synthetic mineral $Sr_2[UO_2(CO_3)_3] \times 8H_2O$ shows some deviations especially in the lower wavelength range. The fluorescence lifetimes of all these minerals are longer than 16 μs, whereas the solution species show lifetimes in the nanosecond range.

Time-resolved laser-induced fluorescence spectroscopy was used to study the surface of a depleted uranium (DU) disc immersed in a Ca–phosphate solution for 182 days [86]. The weathering solution contained, among others, 2.49×10^{-3} M calcium and 1.05×10^{-3} M phosphate, representing pore water concentrations of agricultural soils. By comparison of the TRLFS spectra it was shown that meta-autunite, a uranium(VI) phosphate, has formed during the low temperature alteration on the DU disc. This secondary uranium(VI) mineral phase was identified, at least in a fingerprinting procedure, by comparing it with TRLFS-spectra from an in-house uranium(VI) TRLFS database, including uranium(VI) oxides, uranium(VI) hydroxides, uranium(VI) sulfates and also uranium(VI) phosphates. Six fluorescence emission bands at 486, 501, 522, 546, 573 and 601 nm, and two fluorescence lifetimes of 50 ± 5 and 700 ± 25 ns characterize the TRLFS-spectrum.

Stumpf et al. [87] reports the sorption of curium onto smectite and kaolinite. At low pH an outer sphere complex was detected by fluorescence spectroscopy. With increasing pH an inner sphere adsorption via aluminol edge site occur. The species detected on the surface of clay minerals were assigned to be $a{\equiv}Al{-}O{-}Cm^{2+}{-}(H_2O)_5$ and at higher pH $a{\equiv}Al{-}O{-}Cm^{+}(OH){-}(H_2O)_4$ or a bidentate species $a{\equiv}(Al{-}O)_2{-}Cm^{+}{-}(H_2O)_5$. The sorption behaviour of Cm(III) onto γ-alumina was also studied [88]. Here the same types of species were detected. However, the peak maxima for the first species differ slightly (598.8 and 601.2 nm, respectively). In the case of the interaction with calcite it was shown that curium is

incorporated into the crystal lattice of calcite [89]. The authors came to this conclusion by studying the spectroscopic shift of the fluorescence signal and the increase of the fluorescence decay time of the curium species formed. As clearly multi-exponential fluorescence decays were observed, changes of the equilibria between the several species in the excited state are not expected. Some structural suggestions on the environment of the curium ion on the surface and inclusions in the calcite lattice are given, explained by the increase of the fluorescence decay time to 314 and 1302 μs. These fluorescence lifetimes correlate to Cm species with one and no water molecules in the solvation shell.

6. Outlook

Laser-induced spectroscopic methods have been widely established in actinide chemistry due to their extreme high sensitivity. New applications such as low temperature measurements, spectroscopy of interactions with organic ligands as well as the possibility to detect short living fluorescent actinide species (protactinium(IV), uranium(IV) and americium(III)) are expressions of great interest in actinide chemistry at very low concentrations and in direct speciation techniques.

Acknowledgements

The author thanks Prof. G. Bernhard for many fruitful discussions during the preparation of this review. He also wishes to thank V. Brendler and Th. Arnold for enquiry of some literature.

References

[1] J.V. Beitz, J.P. Hessler, Nucl. Technol. 51 (1980) 169.
[2] W. Schrepp, R. Stumpe, J.I. Kim, H. Walther, Appl. Phys. B32 (1983) 207.
[3] J.I. Kim, in: A.J. Freeman, C. Keller (Eds.), Handbook of the Physics and Chemistry of the Actinides, vol. 4, Elsevier Science Publishers B.V., 1986, p. 413.
[4] J.V. Beitz, D.L. Bowers, M.M. Doxtander, V.A. Maroni, D.T. Reed, Radiochim. Acta 44/45 (1988) 87.
[5] J.I. Kim, R. Stumpe, R. Klenze, Top. Curr. Chem. 157 (1990) 129.
[6] R. Klenze, J.I. Kim, H. Wimmer, Radiochim. Acta 52/53 (1991) 97.
[7] G. Geipel, G. Bernhard, V. Brendler, H. Nitsche, Radiochim. Acta 82 (1998) 59.
[8] G. Geipel, M. Acker, D. Vulpius, G. Bernhard, H. Nitsche, Th. Fanghänel, Spectrochim. Acta A 60 (2004) 417.
[9] D.A. Wruck, C.E.A. Palmer, R.J. Silva, Report UCRL-JC-125198 (1996).
[10] R.J. Silva, G. Bidoglio, M.H. Rand, P. Robouch, H. Wanner, I. Puigdomenech, Chemical Thermodynamics, vol. 2, Chemical Thermodynamics of Americium; NEA-OECD, Elsevier, New York, 1995.
[11] J.I. Kim, G. Buckau, E. Bryant, R. Klenze, Radiochim. Acta 48 (1989) 135.
[12] J.I. Kim, D.S. Rhee, G. Buckau, Radiochim. Acta 52/53 (1991) 49.
[13] G. Buckau, Komplexierung von Americium(III) mit Huminstoffen in natürlichen Gewässern, Dissertation, Fachbereich Chemie, Freie Universität Berlin, 81991, p. 79.
[14] G. Geipel, G. Bernhard, V. Brendler, in: B.-J. Merkel, B. Planer-Friedrich, Chr. Wolkersdorfer (Eds.), Uranium in the Aquatic Environment, Springer Verlag, Berlin, Heidelberg, 2002, p. 373.
[15] C. Mesmin, D. Roudil, A. Hanssens, Ch. Madic, Radiochim. Acta 91 (2003) 385.
[16] V. Balzani, F. Bolleta, M.T. Gandolfi, M. Maestri, Top. Curr. Chem. 75 (1978) 1.64.
[17] G. Bernhard, G. Geipel, V. Brendler, H. Nitsche, Radiochim. Acta 74 (1996) 87.
[18] G. Bernhard, G. Geipel, V. Brendler, H. Nitsche, J. Alloys Compd. 271/273 (1998) 201.
[19] G. Bernhard, G. Geipel, T. Reich, V. Brendler, S. Amayri, H. Nitsche, Radiochim. Acta 89 (2001) 511.
[20] S. Amayri, T. Reich, Th. Arnold, G. Geipel, G. Bernhard, J. Solid State Chem. 178 (2005) 567.
[21] T. Kimura, R. Nagaishi, Y. Kato, Z. Yoshida, Radiochim. Acta 89 (2001) 125.
[22] Z. Wang, J.M. Zachara, W. Yantasee, P.L. Gassman, C. Liu, A.G. Joly, Environ. Sci. Technol. 38 (2004) 5591.
[23] R. Guillaumont, Th. Fanghänel, J. Fuger, I. Grenthe, V. Neck, D.A. Palmer, M.H. Rand, Chemical Thermodynamics 5, Update of the Chemical Thermodynamics of Uranium, Neptunium Plutonium Americium and Technetium, Elsevier, Amsterdam, 2003.
[24] F.J. Pearson, U. Berner, NAGRA Thermochemical data base I. Core Data, NAGRA Technical Report 91-17, 1991.
[25] F.J. Pearson, U. Berner, W. Hummel, NAGRA Thermochemical data base II Suplemental Data 05/92, NAGRA Technical Report 91-1, 1992.
[26] Z. Wang, J.M. Zachara, J.P. Mc Kinley, St.C. Smith, Environ. Sci. Technol. 39 (2005) 2651.
[27] T. Kimura, R. Nagashi, T. Ozaki, M. Arisaka, Z. Yoshida, J. Nucl. Sci. Techn. 3 (Suppl.) (2002) 233.
[28] A. Kirishima, T. Kimura, O. Tochiyama, Z. Yoshida, J. Alloys Compd. 374 (2004) 277.
[29] G. Geipel, S. Nagasaki, S., Annual report 2002, Institute of Radiochemistry, FZR-373, 2003, p. 9.
[30] G. Geipel, S. Nagasaki, Annual report 2003, Institute of Radiochemistry, FZR-400, 2004, (p. 1 and 6).
[31] I. Billard, K. Lützenkirchen, Radiochim. Acta 91 (2003) 285.
[32] A. Weller, Naturwissenschaften 42 (1955) 175.
[33] D. Vulpius, G. Geipel, L. Baraniak, G. Bernhard, Spectrochim. Acta A in press, http://authors.elsevier.com/sd/article/S1386142505002969.
[34] M.M. Puchalski, M.J. Morra, R. von Wandruszka, Fresen. J. Anal. Chem. 340 (1991) 341.
[35] D.F. Eaton, Pure Appl. Chem. 62 (1990) 1631.
[36] D.L. Perry, S.M. Klainer, H.R. Bowman, F.P. Milanovich, T. Hirschfeld, S. Miller, Anal. Chem. 53 (1981) 1048.
[37] C. Moulin, I. Laszak, V. Moulin, C. Tondre, Appl. Spectrosc. 52 (1998) 528.
[38] H. Wimmer, R. Klenze, J.I. Kim, Radiochim. Acta 56 (1992) 79.
[39] H. Wimmer, J.I. Kim, R. Klenze, Radiochim. Acta 56 (1992) 165.
[40] P. Thouvenot, S. Hubert, C. Moulin, P. Decambox, P. Mauchien, Radiochim. Acta 61 (1993) 15.
[41] C.M. Marquardt, P.J. Panak, C. Apostolidis, A. Morgenstern, C. Walther, R. Klenze, Th. Fanghänel, Radiochim. Acta 92 (2004) 445.
[42] A. Kirishima, T. Kimura, O. Tochiyama, Z. Yoshida, Chem. Commun. (2003) 910.
[43] A. Kirishima, T. Kimura, R. Ngaishi, O. Tochiyama, Radiochim. Acta 92 (2004) 705.
[44] G. Meinrath, Y. Kato, Z. Yoshida, J. Radioanal. Nucl. Chem. 174 (1993) 299.
[45] Y. Kato, G. Meinrath, T. Kimura, Z. Yoshida, Radiochim. Acta 64 (1994) 107.
[46] V. Eliet, G. Bidoglio, N. Omenetto, L. Parma, I. Grenthe, J. Chem. Soc. Faraday Trans. 91 (1995) 2275.
[47] V. Eliet, I. Grenthe, G. Bidoglio, Appl. Spectrosc. 54 (2000) 99.
[48] G. Geipel, A. Brachmann, V. Brendler, G. Bernhard, H. Nitsche, Radiochim. Acta 75 (1996) 199.
[49] H. Moll, T. Reich, Ch. Hennig, A. Rossberg, Z. Szabo, I. Grenthe, Radiochim. Acta 88 (2000) 559.
[50] S. Scapolan, E. Ansoborlo, C. Moulin, C. Madic, J. Alloys Compd. 271/273 (1998) 106.
[51] V. Brendler, G. Geipel, G. Bernhard, H. Nitsche, Radiochim. Acta 74 (1996) 75.

[52] J. De Pablo, private communication (2005), article for Radiochim. Acta in preparation.
[53] G. Geipel, G. Bernhard, V. Brendler, T. Reich, NRC5, in: Proceedings of the 5th International Conference on Nuclear and Radiochemistry, Extended Abstracts, Pontresina, Switzerland, 3–8 September, 2000, p. 473.
[54] A. Koban, G. Geipel, G. Bernhard, Radiochim. Acta 91 (2003) 393.
[55] A. Koban, G. Bernhard, Polyhedron 23 (2004) 1793.
[56] A. Koban, G. Geipel, A. Rossberg, G. Bernhard, Radiochim. Acta 92 (2004) 903.
[57] M. Rutsch, G. Geipel, V. Brendler, G. Bernhard, H. Nitsche, Radiochim. Acta 86 (1999) 135.
[58] G. Geipel, G. Bernhard, M. Rutsch, V. Brendler, H. Nitsche, in: T.E. Baca, T. Florkowski (Eds.), The Environmental Challenges of Nuclear Disarmament, Kluwer Academic Publishers, 2000, p. 323.
[59] S. Amayri, G. Geipel, T. Reich, W. Matz, G. Bernhard, NRC5, in: Proceedings of the 5th International Conference on Nuclear and Radiochemistry, Extended Abstracts, Pontresina, Switzerland, 3–8 September, 2000, p. 404.
[60] S.N. Kalmykow, G.R. Choppin, Radiochim. Acta 88 (2000) 603.
[61] W.DeW. Horrocks, D.R. Sudnick, J. Amer. Chem. Soc. 101 (1979) 334.
[62] T. Kimura, Y. Kato, J. Alloys Compd. 271/273 (1998) 867.
[63] T. Kimura, G.R. Choppin, J. Alloys Compd. 213/214 (1994) 313.
[64] Th. Fanghänel, J.I. Kim, P. Paviet, R. Klenze, W. Hauser, Radiochim. Acta 66/67 (1994) 91.
[65] P. Paviet, Th. Fanghänel, R. Klenze, J.I. Kim, Radiochim. Acta 74 (1996) 99.
[66] Th. Fanghänel, H.T. Weger, Th. Könnecke, V. Neck, P. Paviet-Hartmann, E. Steinle, J.I. Kim, Radiochim. Acta 82 (1998) 47.
[67] H. Moll, G. Geipel, G. Bernhard, Inorg. Chim. Acta 358 (2005) 2275.
[68] L.D. Pettit, K.J Powell, Stability Constants Database (SC-Database), Academic Software, Sourby Old Farm, Timble, Otley, http://www.acadsoft.co.uk, 2001.
[69] E.N. Rizkalla, F. Netoux, S. Dabod-Seignon, M. Pages, J. Inorg. Biochem. 51 (1993) 701.
[70] G.R. Choppin, Radiochim. Acta. 32 (1983) 43.
[71] Th. Fanghänel, H.T. Weger, G. Schubert, J.I. Kim, Radiochim. Acta 82 (1998) 55.
[72] P. Panak, R. Klenze, J.I. Kim, H. Wimmer, J. Alloys Compd. 225 (1995) 261.
[73] R. Klenze, P. Panak, J.I. Kim, J. Alloys Compd. 271/273 (1998) 746.
[74] P.J. Panak, R. Knopp, C.H. Booth, H. Nitsche, Radiochim. Acta 90 (2002) 779.
[75] M. Merroun, Ch. Hennig, A. Rossberg, G. Geipel, T. Reich, S. Selenska-Pobell, Biometals (2002) 669.
[76] A. Günther, G. Bernhard, G. Geipel, T. Reich, A. Rossberg, H. Nitsche, Radiochim. Acta 91 (2003) 319.
[77] T. Ozaki, J.B. Gillow, A.J. Francis, T. Kimura, T. Ohnuki, Z. Yoshida, J. Nucl. Sci. Technol. 3 (Suppl.) (2002) 950.
[78] H. Moll, Th. Stumpf, M. Merroun, A. Rossberg, S. Selenska-Pobell, BernhardF G., Environ. Sci. Technol. 38 (2004) 1455.
[79] I. Billard, in: K.A. Gschneidner Jr., J.-C.G. Bünzli, V.K. Pecharsky (Eds.), Handbook on the Physics and Chemistry of Rare Earths, Elsevier Science Publishers, 2004, p. 465.
[80] R. Vochten, L. van Haverbeke, K. van Springel, Can. Minerl. 31 (1993) 167.
[81] R. Vochten, L. van Haverbeke, K. van Springel, N. Jb. Miner. Mh. (1995) 470.
[82] R. Vochten, N. Blaton, O. Peeters, K. van Springel, L. van Haverbeke, Can. Mineral. 35 (1997) 735.
[83] G. Geipel, G. Bernhard, M. Rutsch, V. Brendler, H. Nitsche, Radiochim. Acta 88 (2000) 757.
[84] S. Amayri, T. Arnold, H. Foerstendorf, G. Geipel, G. Bernhard, Can. Mineral. 42 (2004) 953.
[85] S. Amayri, T. Arnold, T. Reich, H. Foerstendorf, G. Geipel, G. Bernhard, A. Massanek, Environ. Sci. Technol. 38 (2004) 6032.
[86] N. Baumann, T. Arnold, G. Geipel, E. Trueman, S. Black, D. Read, Technical note, J. Total Environ. in press, available at www.sciencedirect.com, doi:10.1016/j.scitotenv.2005.09.093.
[87] Th. Stumpf, S. Bauer, F. Coppin, J.I. Kim, Environ. Sci. Technol. 35 (2001) 3691.
[88] Th. Stumpf, Th. Rabung, R. Klenze, H. Geckeis, J.I. Kim, J. Colloid Interf. Sci. 238 (2001) 219.
[89] Th. Stumpf, Th. Fanghänel, J. Colloid Interf. Sci. 249 (2002) 119.